Microporous and Mesoporous Materials 190 (2014) 301–308

Contents lists available at ScienceDirect

Microporous and Mesoporous Materials

journal homepage: www.elsevier.com/locate/micromeso

Hydrogen-selective natural mordenite in a membrane reactor for ethane dehydrogenation

A.M. Avila, Z. Yu, S. Fazli, J.A. Sawada, S.M. Kuznicki *

Department of Chemical and Materials Engineering, University of Alberta, Edmonton, Alberta T6G 2V4, Canada

ARTICLE INFO

Article history:
Received 31 October 2013
Received in revised form 10 January 2014
Accepted 12 February 2014
Available online 26 February 2014

Keywords:
Natural zeolite
Mordenite
Ethane dehydrogenation
Membrane reactor
Ethylene

ABSTRACT

Lab-scale ethane dehydrogenation experiments with natural mordenite disks in a membrane reactor showed an increase in ethane conversion and ethylene yield compared to their equilibrium values. Experiments performed with larger membrane permeation area confirmed the trend that higher conversions are expected as the ratio of product permeation and product formation rates increases. Using the lab-scale membrane reactor module an ethylene yield enhancement of ~17% was observed at 500 °C. At a higher reaction temperature (550 °C), ethane dehydrogenation experiments resulted in a ~10% ethylene yield enhancement versus ~6% for comparative experiments at 500 °C. At 550 °C the membrane reactor effectiveness improved since the H_2 permeation rate increased proportionally more than its formation rate. This material screening test revealed natural mordenite as a material to be considered in the development of highly-integrated membrane reactor modules for dehydrogenation of alkanes.

1. Introduction

Ethylene is one of the most important petrochemicals in terms of production (156 millions tons in 2012). Ethylene is used as a raw material for producing various polymers such as polyethylene, polyester, polystyrene, polyvinyl chloride and many other intermediate products. Currently, thermal steam cracking is the conventional process technology for ethylene production. Steam-diluted hydrocarbons are decomposed in high temperature cracking furnaces with very short residence time (0.1–0.5 s). The common feedstocks for this process are different grades of naphtha and natural gas components such as ethane and propane. The availability of shale gas nowadays assures that ethane remains the main feedstock for steam cracking in North America.

The dehydrogenation of ethane through thermal steam cracking is an expensive and energy intensive process. Steam cracking process requires high reaction temperatures (800–850 °C) and demands therefore adequate and costly materials and equipment. In addition, because it generates large amounts of coke deposition in the furnace tubes, it requires frequent maintenance. The ethane conversion during steam cracking typically reaches 65–70% and ethylene yield is around 50%. However, further yield improvements are becoming increasingly difficult necessitating the evaluation of new approaches to produce ethylene [1–3].

The membrane reactor concept using inorganic membranes is shown to be a reasonable option for dehydrogenation reactions [4–8]. The dehydrogenation of ethane is endothermic and is limited by the thermodynamic equilibrium. The membrane reactor combines the reaction and separation process in a single step. In this particular reaction, the membrane plays a role as a selective extractor of at least one of the product species. Consequently, the limited-equilibrium reaction is able to shift to the product side.

Despite its potential, there are only few publications dealing with membrane reactor experiments for catalytic ethane dehydrogenation. Champagnie et al. [9] reported experiments of a membrane reactor using a tubular ceramic membrane impregnated with 5 wt% Pt and diluted ethane with hydrogen and argon as feed gas. Gobina and Hughes [10,11] used a Pd–Ag membrane supported on a Vycor glass tube to perform membrane reactor experiments using ethane/N_2 50:50 feed gas mixture and Pt/Al_2O_3 as catalyst. Another report considered a membrane reactor based on an alumina membrane using Pt–Sn/Al_2O_3 and a diluted ethane mixture (10% ethane, 5% H_2, 85% Ar) [12]. All of these previous reports on ethane dehydrogenation using membrane reactors were performed with diluted ethane feeds and as a result, the reported conversions were higher than expected for pure ethane feed at the same reaction temperature. Membranes reactors were also explored for a continuous dosing of O_2 in the oxidative dehydrogenation reaction of ethane. For instance, Lobera et al. [13] used a solid-state oxygen permeable material while Coronas et al. [14] used a porous alumina membrane.

* Corresponding author. Tel.: +1 780 492 8819; fax: +1 780 492 8958.
E-mail address: steve.kuznicki@ualberta.ca (S.M. Kuznicki).

http://dx.doi.org/10.1016/j.micromeso.2014.02.024
1387-1811/

Currently, as process intensification becomes more important there is a need to evaluate new and cost-effective materials capable of taking part in the development of highly compact reactor-separator modules [8]. The application of membrane reactors requires a parallel development of catalyst and membrane materials. The screening tests for membrane materials are required prior to any development step aiming at increasing permeation area. Potential materials to be integrated into membrane reactors require screening and testing experiments in conditions resembling industrial settings. Membrane materials for ethane dehydrogenation should be able to perform at temperatures of 500 °C or higher. Lower reaction temperatures generate low conversion values and thus reduce driving forces across the membrane for product permeation. Material screening methods should consider the parameters affecting the membrane reactor performance. In general, membrane reactor performance has been associated with the Damkohler and membrane Peclet numbers. The Damkohler number is related to the catalyst activity and the Peclet number to the permeation rate characteristics [6,15].

Natural zeolite membranes have shown permselectivity properties in the separation of hydrogen from carbon dioxide and hydrogen from ethane [16,17]. Natural zeolite materials, especially clinoptilolite and mordenite have greater thermal stability and better resistance to harsh chemical conditions than many common commercial synthetic adsorbents [18]. These properties make natural zeolites materials of great interest for testing and integration into a membrane reactor device for ethane dehydrogenation reaction. Natural mordenite is one of the most siliceous natural zeolites. The mordenite framework contains three sets of intersecting channels (A, B, C). The channels A and B are parallel to the *c*-axis and channels C are parallel to the *b*-axis. The channels A are formed by larger, ellipsoidal 12-membered rings (12MRc aperture 0.70×0.65 nm) and by strongly compressed 8-membered rings (8MRc aperture 0.57×0.26 nm). The C channels are also formed by eight-membered rings (8MRb aperture 0.38×0.48 nm) and they link the larger 12MRc channels to the much smaller 8MRc channels. There is no straight connection between the adjacent 12MRc channels. Thus, mordenite behaves as a one-dimensional channel system for diffusion of relatively large molecules. In particular, it has been reported that natural mordenites have adsorption characteristics corresponding to a small-port mordenite [19–23]. Thus, the transport of small hydrocarbons are hindered within the zeolite pores in comparison to the faster diffusing H_2 molecules.

The objective of the work presented here is to evaluate natural mordenite membrane disks in a membrane reactor used for the dehydrogenation of ethane. A material-screening membrane reactor was generated using Pt/Al_2O_3 beads as catalyst and membrane disks coupled to the reaction zone. Outlet molar fractions of reaction species were monitored continually as the reactor system changed between a reactor and membrane reactor mode in situ. The integral mass balance of species as a reactor and membrane reactor mode was considered for the quantification of the reaction rate enhancement. The membrane reactor effectiveness of each experiment was evaluated based on dimensionless numbers that were defined accordingly. The effects of increasing permeation area and reaction temperature were studied comparatively.

2. Experimental

2.1. Catalyst

The catalyst used was 1 wt% Pt, 0.3 wt% Sn supported in Al_2O_3 beads (Alfa Aesar®). The catalyst bead size ranged between 1 and 2 mm. This catalyst was selected after performing activity tests on different catalysts: Cr_2O_3/Al_2O_3, Fe_2O_3, 1 wt% Pt/Al_2O_3 and 1 wt% Pt – 0.3 wt% Sn/Al_2O_3. The selected $Pt–Sn/Al_2O_3$ catalyst showed the highest activity for ethane dehydrogenation at 500 °C.

2.2. Membrane preparation

Natural mordenite membrane disks were prepared from rock material (Paradise Quarry Limited-New Zealand) by sectioning using a diamond saw. Table 1 shows the chemical composition provided by the supplier. Membrane size was 19 mm in diameter, and 1.5 mm in thickness. The discs were polished with a diamond polishing lap (180 mesh, Fac-Ette Manufacturing Inc.) followed by washing in an ultrasonic bath for 30 min. Membrane disks were activated at 750 °C for 4 h before use.

2.3. XRD and SEM characterization

Membrane disks were characterized by X-ray diffraction analysis (XRD) (Rigaku Geigerflex 2173 with a cobalt Co Kα radiation source ($\lambda = 1.79021$ Å) and by scanning electron microscopy (SEM) (Hitachi S2700 equipped with an X-ray EDS detector). XRD patterns for membrane disks treated at different temperatures (25, 550, 650 and 750 °C during 4 h) showed no significant changes which reflect an adequate thermal stability of the material (Fig. 1). SEM images (top and cross-sectional view) of the natural mordenite membrane disks are shown in Fig. 2.

2.4. Membrane permeation tests

The membrane disks were tested using a stainless steel cell and sealed with silicone gaskets. The feed and permeate sides each had a stainless steel tube-shell configuration with an inlet gas flowing through the ¼″ inside tube and an outlet gas flowing through the shell between the ¼″ inside tube and ½″ outside tube [15]. Single gas permeation of hydrogen and ethane were measured at temperatures ranging from 298 to 473 K and feed pressure of 122.0 kPa. Ethylene permeation was measured at 298 K. Argon was used as a sweep gas for the permeate side. The feed side pressure was controlled by a back pressure regulator and the permeate side was kept at ambient pressure. The flow rate of the feed side and the flow rate of the sweep gas (Ar) were kept at 100 mL/min (STP) and 100 mL/min (STP) respectively, throughout the measurements.

Table 1
Chemical composition of natural mordenite (provided by the supplier).

Compound	Weight %
LOI*	15.36
Na_2O	1.60
MgO	0.568
Al_2O_3	9.382
SiO_2	56.42
P_2O_5	0.115
SO_3	0.0796
K_2O	0.70
CaO	12.24
TiO_2	0.269
Cr_2O_3	0.0035
MnO	0.0715
Fe_2O_3	2.49
NiO	0.0034
CuO	0.0038
ZnO	0.0078
Rb_2O	0.0015
SrO	0.0401
Y_2O_3	0.0052
ZrO_2	0.011

* LOI = loss on ignition at 950 °C for 1 h.

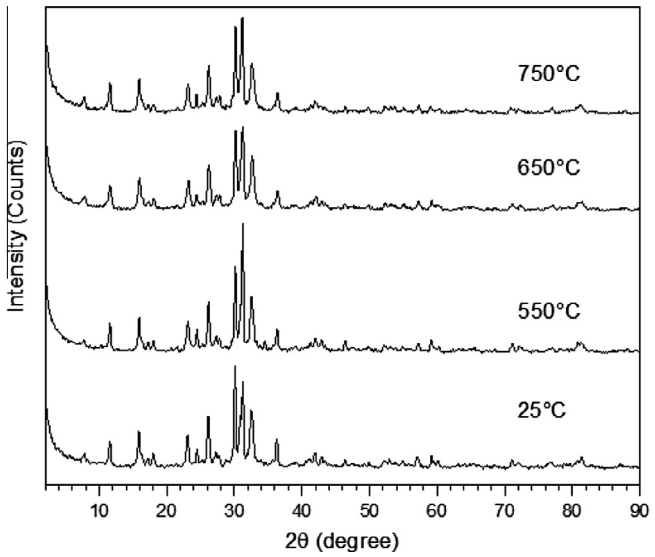

Fig. 1. XRD patterns for natural mordenite membrane surface: membrane disk samples treated at 25, 550, 650 and 750 °C during 4 h.

The permeation system was placed into a tube furnace with a multipoint programmed temperature controller. For the gas composition analysis, an on-line gas chromatograph (GC; Shimadzu GC-14B) with a HayeSep Q packed column and a thermal conductivity detector was used.

2.5. Membrane reactor setup

The membrane reactor configuration is shown in Fig. 3. The outer tube is made of quartz (ID = 22 mm) and corresponds to the reaction side of the membrane reactor. The permeate side consists of two concentric ceramic tubes. The sweep gas flows through the inner tube and the permeate flux flows out through the outer tube (12.6 mm OD). The catalyst beads were packed in the feed side in contact to the membrane. The membrane was sealed on the end of the ceramic outer tube by using high temperature ceramic adhesive (REFRACTOBOND ALP, Accumet Materials Co.) following the curing procedures.

2.6. Experimental conditions

Reaction experiments were performed at 500 and 550 °C. The catalyst amount used in each run was 2.2 g. An on-line GC (Bruker 450-GC) with automatic sampling valves and TCD detector was used to analyze both permeation side and the reaction side streams. Inlet flow rates (feed and sweep gas) were controlled by mass flow controllers (Sierra Instruments Inc.). Outlet flow rates (from reaction and permeate sides) were measured by soap film meters under lab conditions (25 °C, 101.3 kPa). Ethane (99.8%) was fed into the reactor with a flow rate set up at 12.0 mL/min (25 °C, 101.3 kPa). Argon (99.9%) with a flow rate set up at 54.0 mL/min (25 °C, 101.3 kPa) was used as a sweep gas. The increase of sweep gas flow rate beyond 54.0 mL/min did not improve the hydrogen removal. Feed pressure was maintained at 104.0 kPa with a back pressure regulator valve while permeate pressure was atmospheric (101.3 kPa). Argon was not detected in the retentate stream when pure helium was used as a feed stream in the membrane reactor at the same operating conditions. Thus, feed dilution effects were negligible in the membrane reactor experiments. The carbon mass balance closures for all the experiments were within 99 ± 1% without considering the coke formation.

2.7. Switching from a membrane reactor to a reactor mode

In order to quantify the enhancement of the ethane conversion, the membrane reactor performance requires to be compared to that of a packed bed reactor at the same operating conditions. Small changes of variable conditions between both experiments can hinder a fair comparison. Different catalyst activities, slight deviations in feed rate and pressure drop across membranes are a few of the variables affecting the data comparison. Therefore, better comparable data can be obtained using the same experiment rather than two different experiments.

By shutting the sweep gas off (inlet and outlet), the system switches from a membrane reactor mode (MR) towards a reactor mode (R) (Fig. 4). Partial pressures of reactant species increase in the permeate side until they equilibrate with those in the reaction side. The membrane stops working as a product extractor and the system essentially behaves as a packed bed reactor. Following this procedure, a fair comparison can be made between both system modes: reactor and membrane reactor.

2.8. Mass balance of species as a reactor and membrane reactor mode

The reaction rate enhancement achieved when the systems switches between the different modes can be quantified considering the mass balance of species in the reaction zone. The integral form of the continuity equation for the species i in steady-state conditions can be expressed as

$$\int_{A_R} \bar{N}_i \cdot \bar{n}\, dA = W \int_{V_R} r_i^*\, dV \tag{1}$$

where the term on the left-hand side represents the net molar flow rate of species i through the boundaries of the reaction zone, r_i^* is the local reaction rate in mol/cm^3 g_{cat} s and W is the catalyst amount in the reactor. Then, Eq. (1) reduces to

$$F_{i,\text{out}} - F_{i,\text{in}} = W\langle r_i^* \rangle_{V_R} \tag{2}$$

where F_i is the molar flow rate of each reacting species and $\langle r_i^* \rangle_{V_R}$ is the volume-integrated reaction rate in mol/g_{cat} s.

The integral mass balance was applied for each product species of ethane dehydrogenation (H_2 and C_2H_4) as both reactor and membrane reactor mode. The combination of each resulting expression gives

$$\frac{\langle r_i^* \rangle_{V_{R,MR}}}{\langle r_i^* \rangle_{V_{R,R}}} = \frac{[Q_{\text{out}} x_{i,\text{out}}]_{MR}}{[Q_{\text{out}} x_{i,\text{out}}]_R} + \frac{[Q_p x_{i,p}]}{[Q_{\text{out}} x_{i,\text{out}}]_R} \tag{3}$$

Eq. (4) can also be expressed in terms of dimensionless numbers

$$\tau_{i,MR/R} = \gamma_{i,MR/R} + \beta_{i,P/R} \tag{4}$$

where $\tau_{i,MR/R}$ is the reaction rate ratio of product species between MR and R mode, $\gamma_{i,MR/R}$ is the outlet flow rate ratio for product species between the MR and the R mode and $\beta_{i,P/R}$ is the ratio between product permeation flow rate over its formation rate in the R mode. The dimensionless number $\tau_{i,MR/R}$ represents the reaction rate enhancement achieved by the system as it switches from R to MR mode. It can be estimated in terms of the flow rate leaving the reaction zone, Q_{out}; the outlet permeate flow rate, Q_p and the outlet compositions from the reaction and permeate zones, $x_{i,out}$ and $x_{i,p}$.

All the dimensionless numbers defined for the analysis of the experimental data are summarized in Table 2. They were also related to the Damkohler and membrane Peclet numbers estimated in reaction conditions [24]. The Damkohler number relates the rate of reaction to the rate of reactant feed. The membrane Peclet number is defined in terms of the reactant feed rate and permeation rate of each product.

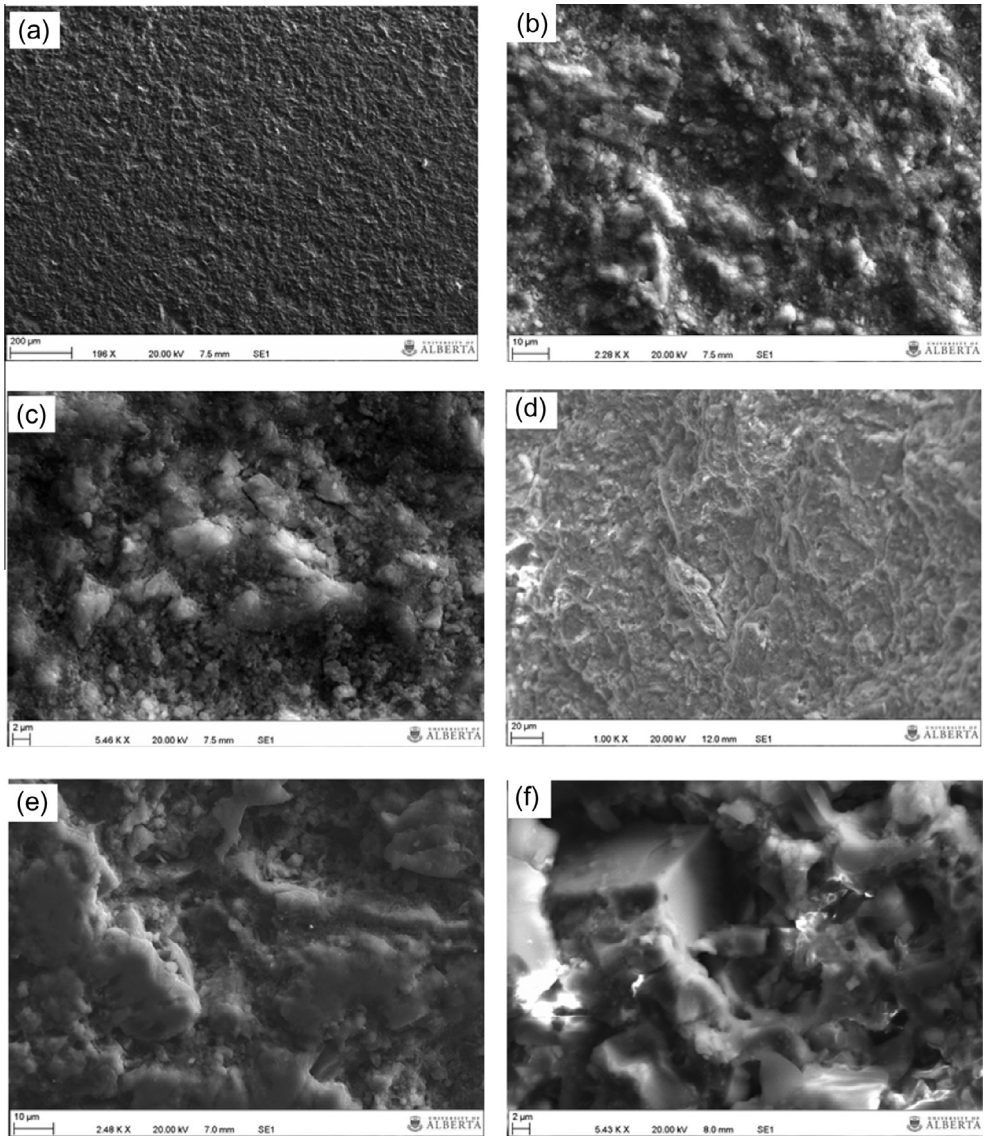

Fig. 2. SEM images of natural mordenite membrane: (a), (b), and (c) are top views (scale bar = 200, 10, and 2 μm, respectively; (d), (e), and (f) are cross-sectional view (scale bar = 20, 10, and 2 μm).

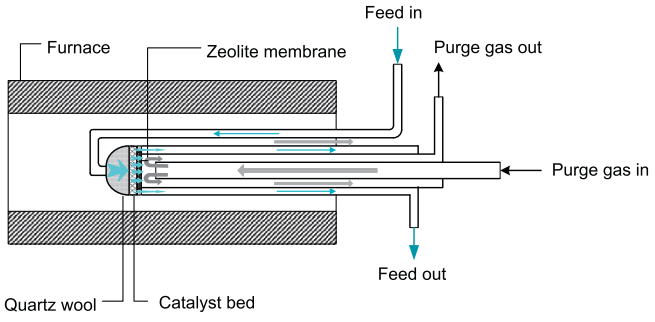

Fig. 3. Membrane reactor lab setup.

The reaction enhancement can also be evaluated using ethane conversion, ethylene yield and ethylene selectivity. Ethane conversion was calculated in terms of the reaction products. For the reactor mode the ethane conversion is expressed as

$$\alpha_{C_2} = \left(1 - \frac{x_{C_2,\text{out}}}{x_{C_2,\text{out}} + x_{C_2^=,\text{out}} + \frac{1}{2}x_{CH_4,\text{out}}}\right).100 \quad (5)$$

where C_2 and $C_2^=$ represent ethane and ethylene species respectively. The ethylene yield was also quantified accordingly.

$$Y_{C_2^=} = \left(\frac{x_{C_2^=,\text{out}}}{x_{C_2,\text{out}} + x_{C_2^=,\text{out}} + \frac{1}{2}x_{CH_4,\text{out}}}\right).100 \quad (6)$$

And then, ethylene selectivity can be expressed as:

$$S_{C_2^=} = \frac{Y_{C_2^=}}{\alpha_{C_2}} = \left(\frac{x_{C_2^=,\text{out}}}{x_{C_2^=,\text{out}} + \frac{1}{2}x_{CH_4,\text{out}}}\right).100 \quad (7)$$

3. Results and discussion

3.1. H_2/C_2H_6 permeance selectivity through natural mordenite membranes

Natural mordenite disks showed permselectivity properties for hydrogen over ethane. Due to the thermal stability of this material,

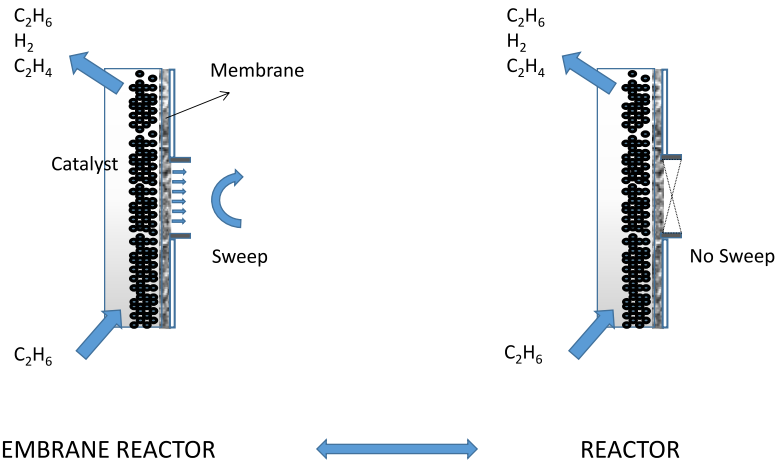

Fig. 4. Outline of the different operating modes (membrane reactor and reactor mode) for the experiments of ethane dehydrogenation.

Table 2
Dimensionless numbers defined for the comparison between reactor and membrane reactor mode.

Dimensionless number	Symbol	Definition
Reaction rate ratio	$\tau_{i,MR/R}$	$\tau_{i,MR/R} = \frac{\langle r_i^* \rangle V_{R,MR}}{\langle r_i^* \rangle V_{R,R}}$
Outlet flow rate ratio	$\gamma_{i,MR/R}$	$\gamma_{i,MR/R} = \frac{[Q_{out} x_{i,out}]_{MR}}{[Q_{out} x_{i,out}]_R}$
Permeation-reaction rate ratio	$\beta_{i,P/R}$	$\beta_{i,P/R} = \frac{[Q_P x_{i,P}]}{[Q_{out} x_{i,out}]_R} = \frac{1}{Da_R P_e}$ *
H_2/ethane outlet molar ratio	φ_{H_2/C_2}	$\varphi_{H_2/C_2} = \frac{x_{H_2,out}}{x_{C_2,out}}$

* $Da_R = \frac{\langle r_i^* \rangle V_{R,R} W}{F_{in}}$; $\frac{1}{P_e} = \frac{F_{i,P}}{F_{in}}$.

the permselectivity properties are relevant as temperature increases. Fig. 5 shows the H_2 and C_2H_6 permeances through mordenite disks as a function of temperature. H_2 permeance was higher than ethane permeance. The H_2/C_2H_6 selectivity at 200 °C was 6.0. The selectivity values were higher than Knudsen selectivity ($S^K_{H_2/C_2H_6} = 3.9$) throughout the temperature range of measurement.

Both H_2 and C_2H_6 permeances did not decrease as temperature increased indicating that zeolitic flux contribution prevails at the test conditions. H_2 permeance increased slightly with the increase in temperature indicating more zeolitic flux contribution than C_2H_6. As shown previously in the characterization of natural zeolite membranes [15], a higher fraction of H_2 total flux passes through the zeolite crystals as the temperature increases. On the contrary, the nonselective fraction related to the flux through relatively large nonzeolite pores (viscous flux) decreases with temperature. Thus, the selective fraction of H_2 permeance able to provide separation selectivity increases with temperature.

Comparative permeation tests through the mordenite disks at 25 °C produced an ethylene permeance of 2.0×10^{-8} mol/m^2 s Pa compared to 2.7×10^{-8} mol/m^2 s Pa for ethane. Ethylene permeance is expected to be lower than ethane due to its stronger adsorption affinity on zeolitic materials. The stronger interactions of ethylene molecules with the adsorption sites in the zeolite micropores are associated with their π-bonds [25,26].

3.2. Reversibility in the reactor-membrane reactor mode

The system started as a membrane reactor mode (MR) when the sweep gas was on (Fig. 6). It switched toward a reactor mode (R) as the sweep gas was shut off. At this point, the membrane stops working as a product extractor and H_2 molar fraction increased while ethylene value decreased. Then, the system returned to the MR mode as the sweep gas was switched on again. The molar fraction profiles went back gradually to the former steady-state values. The dynamics of catalyst deactivation was slow in comparison to the characteristic times of the process: residence time, reaction time and permeation time. The observed data reflected the system's reversibility when switching back and forth between R and MR modes. The system was able to capture molar fraction changes

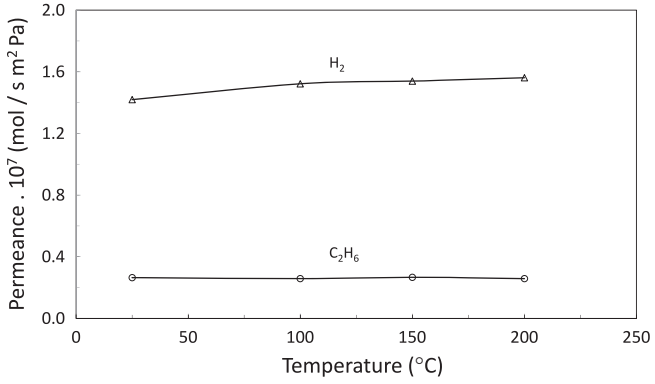

Fig. 5. H_2 and C_2H_6 permeances through natural mordenite disks as a function of temperature. Feed side pressure: 122.0 kPa. Permeate side pressure: 101.3 kPa.

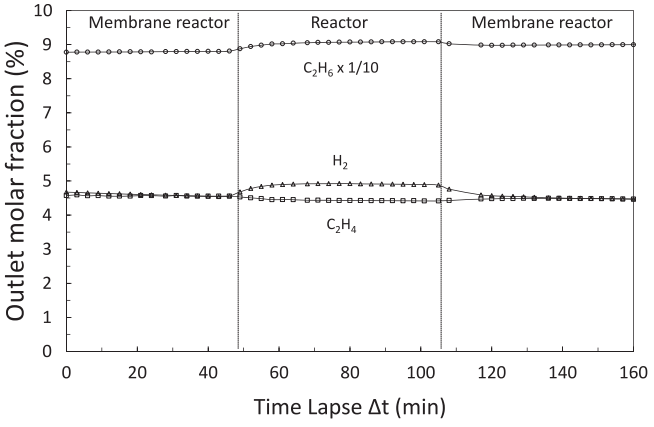

Fig. 6. Dynamics of molar fractions of hydrogen, ethylene and ethane in the reactor outlet as the system switches reversibly between a membrane reactor and a reactor operating mode. Ethane dehydrogenation reaction at 500 °C. WHSV = 0.4 h^{-1}.

of the species leaving the reaction zone as it switched between the two different operating modes.

3.3. Reactor and membrane reactor modes: dynamics of molar fractions of reaction species in the reactor outlet

When ethane is fed into the membrane reactor, the molar fraction composition leaving the reaction zone gradually changes until reaching a quasi-steady state condition in the membrane reactor mode (MR) (Fig. 7a). At this point, the system is switched to the reactor mode (R). As a consequence, the exit molar fractions change until reaching a new quasi-steady state corresponding to the R mode. H_2 molar fraction increased from 4.5% at the MR up to 4.8% at the R mode (Fig. 7b). During the MR–R transition, H_2 molar fraction increased since H_2 stops permeating across the membrane building up partial pressure in the reaction side. Ethylene molar fraction in R mode decreased approaching the corresponding equilibrium value calculated with thermodynamic data. Ethylene molar fraction, thus, was higher in the MR mode than at the R mode. As shown in Table 3, the reaction rate ratio, $\tau_{C_2^=,MR/R}$, calculated with Eq. (5) in terms of ethylene was 1.05. This reflects that ethylene yield is higher at the MR mode than at the R mode. The ethylene yields calculated with Eq. (7) were $Y_{C_2^=}$ = 4.6% in the R mode and $Y_{C_2^=}$ = 4.9% in the MR mode. This represents an ethylene yield enhancement of 6.0%. Molar fraction of ethane in R mode also approaches the value predicted by the thermodynamic equilibrium of the reaction. In the MR mode, however, the ethane molar fraction was lower than the equilibrium because more ethane is converted in these conditions and also because of a fraction permeating across the membrane. Ethane conversion increased from 4.9% (in the R mode) up to 5.2% (in the MR mode) (Table 3). Methane was the side-reaction product and their corresponding selectivity values are also shown in Table 3.

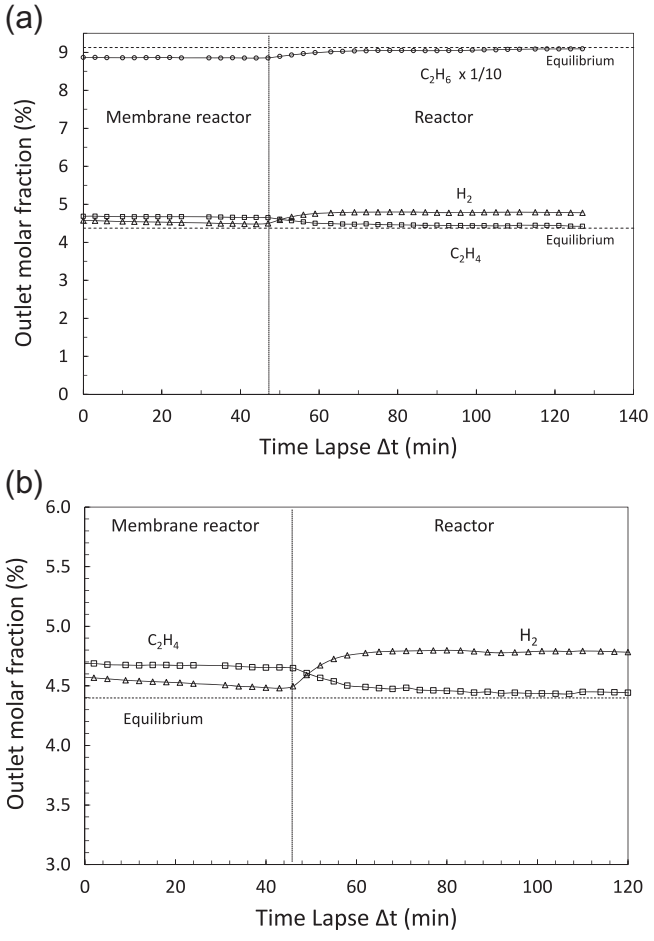

Fig. 7. Dynamics of outlet molar fractions of: (a) reaction species (ethane, hydrogen and ethylene) and (b) hydrogen and ethylene for the membrane reactor switching to reactor mode at 500 °C. Dashed lines represent molar fractions of species calculated with thermodynamic equilibrium data. WHSV = 0.4 h^{-1}. Outlet flow rates [mL/min] (25 °C, 101.3 kPa): $[Q_{out}]_{MR}$ = 12.6; $[Q_{out}]_R$ = 12.9. Permeate rate: 55.0. Permeate composition [%v/v]: $x_{H_2,out}$ = 0.19; $x_{C_2^=,out}$ = 0.025; $x_{C_2,out}$ = 0.69.

The conversion enhancement in this experiment can be analyzed in terms of the H_2 permeation rate in relation to its formation rate. The permeation/reaction rate ratio, $\beta_{H_2,P/R}$, was 16%. This means that ~16% of the H_2 formed in the reaction is extracted through the membrane. Statistically, membrane reactor experiments for different types of hydrogen forming reactions show that the percentage of conversion enhancement is usually not higher than the percentage of H_2 removal in relation to its formation rate [20]. The value $\beta_{H_2,P/R} = 16\%$ is equivalent to a Damkohler–Peclet number $Da_R P_e$ = 6.1. This number is far from its optimal value ($Da_R P_e \sim 1$) in terms of a membrane reactor effectiveness [13]. A $Da_R P_e$ number approaching one represents a membrane reactor in which all the H_2 generated in the reaction is extracted through the membrane.

3.4. Increasing permeation area/reactor volume $\left(\frac{A}{V_R}\right)$ ratio of the membrane reactor

At the same reaction temperature, 500 °C, another experiment was performed using a membrane with a larger effective area for permeation. As the permeation area in the membrane reactor increased, more H_2 was able to be removed from the reaction system. The H_2 formation rate in the R mode remained the same as the reaction temperature did not change. Therefore, the permeation rate/reaction rate ratio, $\beta_{H_2,P/R}$, increased.

Fig. 8 shows the evolution of the outlet molar fraction profiles of H_2, ethylene and ethane during transition from R mode to MR mode. H_2 molar fraction dropped considerably when the system switched from R to MR mode. The ethylene molar fraction increased from values approaching thermodynamic equilibrium to values higher than those in equilibrium.

For this larger $\frac{A}{V_R}$ ratio membrane reactor ($\frac{A}{V_R}$ = ~0.16), the dimensionless number $\beta_{H_2,P/R}$ was 36% while for the smaller one (A/V = ~0.04), $\beta_{H_2,P/R}$ was 16% (Table 3). Similarly, the ratio φ_{H_2/C_2} (hydrogen/ethane molar ratio at the reactor outlet) decreased up to 80% of its original value when the system switched from R to MR mode. For the lower $\frac{A}{V_R}$ ratio membrane reactor, φ_{H_2/C_2} only decreased from 5.3% as R mode to 5.1% (MR mode). H_2 content in the reaction zone is additionally reduced as the permeation area is larger. Therefore, the reaction rate in the MR mode ($\langle r_i^* \rangle_{V_{R,MR}}$) increased and thus the ethane conversion, α_{C_2}, improved in comparison to a membrane reactor with a smaller permeation area. The corresponding value for the dimensionless number $\tau_{C_2^=,MR/R}$ was 1.15, reflecting a 15% increase in the reaction rate for a MR mode. Ethylene yield improved from 4.4% in the R mode to 5.2% in the MR mode which represents ~17% enhancement.

3.5. Increasing reaction temperature

Similar outlet molar fraction profiles for R and MR modes were obtained when the dehydrogenation reaction was run at higher temperature (550 °C) (Fig. 9). As expected, observed ethane conversions were higher as temperature increased. The ethane conversion for the reactor mode was 9.7%. The conversion calculated from thermodynamic equilibria at 550 °C is 9.2%. The ethylene selectivity at 550 °C was lower than that at 500 °C (Table 3) because as the reaction temperature increased the side reaction effects become

Table 3
Experimental values of the dimensionless numbers defined in Table 1 along with the ethane conversion, α_{C_2}; ethylene yield, $Y_{C_2^=}$; ethylene selectivity, $S_{C_2^=}$, and methane selectivity, S_{CH_4}, for the two operating modes: reactor, R, and membrane reactor, MR. Experiments were performed at 500 °C with an area/reactor volume, $\frac{A}{V_R}$ = 0.04 and 0.16 m^{-1}, and at 550 °C with $\frac{A}{V_R}$ = 0.04 m^{-1}.

Mode	T °C	A/V m^{-1}	$\beta_{H_2,P/R}$ %	φ_{H_2/C_2} %	$\beta_{C_2^=,P/R}$ %	$\tau_{C_2^=,MR/R}$	α_{C_2} %	$Y_{C_2^=}$ %	$S_{C_2^=}$ %	S_{CH_4} %
R	500	0.04	–	5.3	–	–	4.9	4.6	94.0	6.0
MR	500	0.04	16.7	5.1	2.4	1.05	5.2	4.9	94.1	5.9
R	500	0.16	–	5.8	–	–	4.8	4.5	92.4	7.6
MR	500	0.16	36.6	4.6	9.4	1.15	5.5	5.2	94.8	5.2
R	550	0.04	–	11.2	–	–	9.7	9.0	92.2	7.8
MR	550	0.04	24.2	9.9	8.7	1.09	10.5	9.8	93.7	6.3

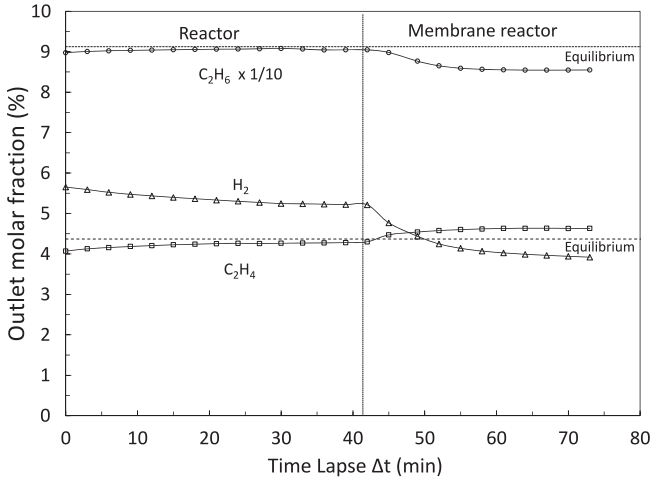

Fig. 8. Dynamics of outlet molar fractions of reaction species (ethane, hydrogen and ethylene) for the reactor mode switching to the membrane reactor mode at 500 °C. Dashed lines represent molar fractions of species calculated with thermodynamic equilibrium data. Membrane reactor with $\frac{A}{V_R}$ = ~0.16. WHSV = 0.4 h^{-1}. Outlet flow rates [mL/min] (25 °C, 101.3 kPa): $[Q_{out}]_{MR}$ = 12.1; $[Q_{out}]_R$ = 12.5. Permeate rate: 55.8. Permeate composition [%v/v]: $x_{H_2,out}$ = 0.43; $x_{C_2^=,out}$ = 0.09; $x_{C_2,out}$ = 1.33.

more important. The reaction rate ratio, $\tau_{C_2^=,MR/R}$, was 1.09. This value was larger than the corresponding value at 500 °C. The ethane conversion at 550 °C increased from 9.7 in the R mode up to 10.5 in the MR mode.

As the ethane conversion increased, the driving force for product permeation increased. Thus, H_2 and ethylene permeate fluxes at 550 °C increased in comparison to experimental data at 500 °C. The dimensionless number $\beta_{H_2,P/R}$ was 24.2% and $\beta_{C_2^=,P/R}$ was 8.7%

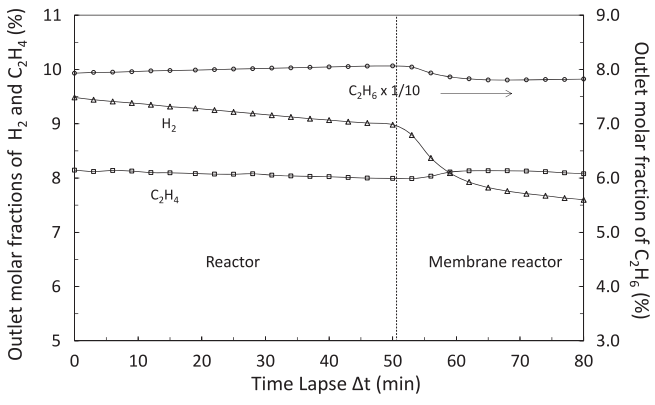

Fig. 9. Dynamics of outlet molar fractions of reaction species (ethane, hydrogen and ethylene) for the reactor mode switching to membrane reactor mode at 550 °C. Ethane molar fraction is read on the right axis. Membrane reactor with area/volume ratio = ~0.04. WHSV = 0.4 h^{-1}. Outlet flow rates [mL/min] (25 °C, 101.3 kPa): $[Q_{out}]_{MR}$ = 12.2; $[Q_{out}]_R$ = 12.4. Permeate rate: 54.2. Permeate composition [%v/v]: $x_{H_2,out}$ = 0.50; $x_{C_2^=,out}$ = 0.16; $x_{C_2,out}$ = 0.60.

Table 4
Ethylene yield enhancements achieved with the membrane reactor at two different reaction temperatures and two $\frac{A}{V_R}$ ratios. The corresponding Damkohler–Peclet numbers were calculated with reaction conditions. WHSV = 0.4 h^{-1}.

Temperature °C	$\frac{A}{V_R}$ m^{-1}	$\frac{1}{P_e}$ (-) × 10^2	Da_R (-) × 10^2	$Da_R P_e$ (-)	$Y_{C_2^=}$ enhancement %
500	0.04	0.82	4.9	6.0	6.1
550	0.04	2.4	10.0	4.1	9.4
500	0.16	2.0	5.4	2.7	16.5

for the experiments performed at 550 °C (Table 3). These values were larger than the corresponding values for the run at 500 °C with the same $\frac{A}{V_R}$ ratio ($\beta_{H_2,P/R}$ = 16.7% and $\beta_{C_2^=,P/R}$ = 2.4%) (Table 3). This effect was also reflected in the φ_{H_2/C_2} ratio. This number decreased from 5.3% to 5.1% (~4% decrease) at 500 °C. However, φ_{H_2/C_2} dropped from 11.2 to 9.9 (~13% drop). In this sense, the increase of reaction temperature provides a positive effect regarding the enhancement of product removal. Ethylene yield increased from 9.0% up to 9.8% which represents a 9.4% enhancement at 550 °C in comparison to 5.3% at 500 °C. Ethylene selectivity rose from 92.2% to 93.7% as shown in Table 3.

3.6. Membrane reactor effectiveness

The experimental results can also be analysed in terms of the Damkohler (Da_R) and Peclet (P_e) numbers. As temperature increased from 500 to 550 °C, the Damkohler number increased two fold as the reaction rate increased with temperature (Table 3). The increase of Da_R is also reflected in the conversion values going from ~5% at 500 °C to ~10% at 550 °C (Table 3). However, the larger formation rate of H_2 was compensated through a higher H_2 removal rate. The H_2 permeation rate was three times larger at 550 °C than at 500 °C. This is reflected in the $\frac{1}{P_e}$ values shown in Table 4. Consequently, the Damkohler–Peclet number ($Da_R P_e$) decreased from 6.0 to 4.1 and thus the effectiveness of the membrane reactor increased. The ethylene yield enhancement at 550 °C was 9.4% which was higher than the 6.1% enhancement at 500 °C. When permeation area increased, the permeation/reaction rate ratio $\beta_{H_2,P/R}$ increased up to 36%. This is equivalent to the $Da_R P_e$ number decreasing down to 2.7. The membrane reactor can work more effectively as $Da_R P_e$ deviates less from 1. The ethylene yield enhanced 17% in these conditions (Table 4). The experiment with a larger H_2 product removal in relation to its formation rate achieved the largest ethylene yield enhancement.

4. Conclusions

Natural mordenite membrane disk coupled to a Pt/Al_2O_3 packed bed reactor formed a membrane reactor that was able to selectively extract H_2 achieving an equilibrium shift of ethane dehydrogenation reaction at 500–550 °C. By increasing the area/volume ratio of the membrane reactor module, a ~17% ethylene

yield enhancement was achieved in comparison to that of packed bed reactor at 500 °C. The effectiveness of the membrane reactor improved since more H_2, in relation to its formation rate, was removed from the system. Membrane reactor experiments at 550 °C showed higher ethylene yield enhancement in comparison to those conducted at 500 °C. At 550 °C the membrane reactor effectiveness increased as the H_2 permeation rate increased more than its formation rate.

With a proper engineering design that accomplishes a high catalyst-membrane interaction in optimal conditions (H_2 permeate rate $\sim$ H_2 formation rate), this cost-effective material can play an important role in the development of efficient membrane reactors modules at high temperatures.

Acknowledgements

The authors thank Albana Zeko for assistance with manuscript edition and Vasily Simanzhenkov and Shahin Goodarznia from NOVA Chemicals Corporation for valuable discussions. Support from the Natural Sciences and Engineering Research Council Industrial Research Chair in Molecular Sieve Separations Technology and Helmholtz-Alberta Initiative are gratefully acknowledged.

References

[1] C.A. Gartner, A.C. van Veen, J.A. Lercher, ChemCatChem 5 (2013) 1–23.
[2] M.J. Skinner, E.L. Michor, W. Fan, M. Tsapatsis, A. Bhan, L.D. Schmidt, ChemSusChem 4 (2011) 1151–1156.
[3] V. Galvita, G. Siddiqi, P. Sun, A.T. Bell, J. Catal. 271 (2010) 209.
[4] P. Liu, M. Sahimi, T. Tsotsis, Curr. Opin. Chem. Eng. 1 (2012) 342–351.
[5] F. Gallucci, E. Fernandez, P. Corengia, M. van Sint, Chem. Eng. Sci. 92 (2013) 40–66.
[6] J. Gascon, F. Kapteijn, B. Zornoza, V. Sebastian, C. Casado, J. Coronas, Chem. Mater. 24 (2012) 2829–2844.
[7] M.O. Daramola, E.F. Aransiola, T.V. Ojumu, Materials 5 (2012) 2101–2136.
[8] S.M. Hashim, A.R. Mohamed, S. Rev. Chem. Eng. 27 (2011) 157–178.
[9] A.M. Champagnie, T.T. Tsotsis, R.G. Minet, I.A. Webster, Chem. Eng. Sci. 45 (1990) 2423–2429.
[10] E. Gobina, R. Hughes, J. Membr. Sci. 90 (1994) 11–19.
[11] E. Gobina, K. Hou, R. Hughes, R. Chem. Eng. Sci. 50 (1995) 2311–2319.
[12] J. Szegner, K.L. Yeung, A. Varma, AIChE J. 43 (1997) 2059–2072.
[13] M.P. Lobera, S. Escolastico, J.M. Serra, Chemcatchem 3 (2011) 1503–1508.
[14] J. Coronas, M. Menéndez, J. Santamaría, Ind. Eng. Chem. Res. 34 (1995) 4229–4234.
[15] S. Battersby, P.W. Teixeira, J. Beltramini, M.C. Duke, V. Rudolph, J.C.D. da Costa, Catal. Today 116 (2006) 12–17.
[16] W. An, P. Swenson, L. Wu, T. Waller, A. Ku, S.M. Kuznicki, J. Membr. Sci. 112 (2011) 414–419.
[17] S.A. Hosseinzadeh Hejazi, A.M. Avila, T.M. Kuznicki, A. Weizhu, S.M. Kuznicki, Ind. Eng. Chem. Res. 50 (2011) 12717–12726.
[18] M.W. Ackley, S.U. Rege, H. Saxena, Microporous Mesopororus Mater. 61 (2003) 25–42.
[19] F. Raatz, C. Marcilly, E. Freund, Zeolites 5 (1985) 329–333.
[20] P. Simoncic, T. Armbruster, Am. Mineral. 89 (2004) 421–431.
[21] M. Ulmanu, I. Anger, in: V.J. Inglezakis, A.A. Zorpas (Eds.), Handbook of Natural Zeolites, Bentham Science Publishers, 2012, pp. 70–102.
[22] B.J. Campbell, T.R. Welberry, R.W. Broach, H.W. Hong, A.K. Cheetham, J. Appl. Crystallogr. 37 (2004) 187–192.
[23] A.F. Masters, T. Maschmeyer, Microporous Mesoporous Mater. 142 (2011) 423–438.
[24] S.T. Oyama, H. Lim, Chem. Eng. Sci. 151 (2009) 351–358.
[25] R.W. Triebe, F.H. Tezel, K.C. Knulbe, Gas Sep. Purif. 10 (1996) 81–84.
[26] M. Shi, A.M. Avila, F. Yang, T.M. Kuznicki, S.M. Kuznicki, Chem. Eng. Sci. 66 (2011) 2817–2822.